Biomedicine & Pharmacotherapy 147 (2022) 112669

Contents lists available at ScienceDirect

Biomedicine & Pharmacotherapy

journal homepage: www.elsevier.com/locate/biopha

Anti-diabetic potential of β-boswellic acid and 11-keto-β-boswellic acid: Mechanistic insights from computational and biochemical approaches

Ajmal Khan [a,1], Imran Khan [b,1], Sobia Ahsan Halim [a], Najeeb Ur Rehman [a], Nasiara Karim [c], Waqar Ahmad [c], Majid Khan [a,d], Rene Csuk [e], Ahmed Al-Harrasi [a,*]

[a] Natural and Medical Sciences Research Center, University of Nizwa, P.O Box 33, Postal Code 616, Birkat Al Mauz, Nizwa, Sultanate of Oman
[b] Department of Pharmacy, University of Swabi, KPK, Pakistan
[c] Department of Pharmacy, University of Malakand, Chakdara 18800, KPK, Pakistan
[d] H. E. J. Research Institute of Chemistry, International Center for Chemical and Biological Sciences, University of Karachi, Karachi 75270, Pakistan
[e] Martin-Luther-University Halle-Wittenberg, Organic Chemistry, Kurt-Mothes-Str. 2, D-06120 Halle (Saale), Germany

ARTICLE INFO

Keywords:
Hypoglycemic
β-Boswellic acid
11-keto-β-boswellic acid
Glibenclamide
Streptozotocin-induced diabetes
Dipeptidyl peptidase 4

ABSTRACT

β-Boswellic acid (β-BA) and 11-keto-β-boswellic acid (β-KBA) are crucial bioactive compounds, mostly isolated from frankincense. These compounds are known for their potent anticancer and anti-inflammatory activities. Herein, we have explored the complete anti-diabetic potential of β-BA and β-KBA with detailed parameters. This research revealed that treatment with β-BA and β-KBA at a dose of 1, 2, and 10 mg/kg body weight for 21 days significantly improved body weight loss, water consumption, and specifically the concentration of blood glucose level (BGL) in diabetic animals, which indicated that the β-BA and β-KBA possess strong anti-diabetic activities. Serum total superoxide dismutase (SOD) and malondialdehyde (MDA) assays were also performed to evaluate the antioxidant effects. The biochemical analysis revealed that these compounds improve an abnormal level of several biochemical parameters like serum lipid values including total cholesterol (TC), triacylglycerol (TG), low-density lipoprotein cholesterol (LDL-C) to a normal level and the high-density lipoprotein cholesterol level (HDL-C). To understand the mechanism of action of β-BA and β-KBA, their most probable biological targets were searched through the inverse docking approach. Our computational analysis reflects that among other probable targets, the Dipeptidyl peptidase 4 (DPP-4) enzyme could be one of the possible binders of β-BA and β-KBA to produce their anti-diabetic activities. These *in-silico* results were validated by an in-vitro experiment. It indicates that the anti-diabetic effects of β-BA and β-KBA are produced by the inhibition of DDP-4. Thus, these anti-diabetic, antioxidant, and anti-hyperlipidemic effects of β-BA and β-KBA suggest these compounds as potential therapeutics for diabetic conditions.

1. Introduction

Diabetes is a long-lasting and serious disease that globally affects individual lives, families, and societies. The global diabetes prevalence in 2019 was estimated to be 9.3% (463 million people) which will increase up to 578 million (10.2%) and 700 million (10.9%) by 2030 and

Abbreviations: AMPK, Activators of 5' adenosine monophosphate-activated protein kinase; ALP, alkaline phosphatase; ALOX5, Arachidonate 5-Lipoxygenase; BGL, blood glucose level; β-BA, β-Boswellic acid; β-KBA, 11-keto-β-boswellic acid; DPP-4, Dipeptidyl peptidase 4; COSY, Correlation spectroscopy; DEPT, Distortionless enhancement by polarization transfer; DS, Docking score; EMA, European Medicines Agency; GIP, gastric inhibitory polypeptide; GDM, Gestational diabetes mellitus; GLP-1, Glucagon-like peptide-1; GPR, G-protein coupled receptor; HMQC, Heteronuclear multiple quantum coherence; HMBC, Heteronuclear multiple bond coherence; HDL, High density lipoprotein; InsR, Insulin receptors; IDF, International Diabetes Federation; LDL, Low density lipoproteins; MDA, malondialdehyde; NMSRC, Natural and Medical Sciences Research Center; PPAR-γ, Peroxisome proliferator-activated receptor gamma; PREP, Prolyl endopeptidase; PTP-1B, Protein-tyrosine phosphatase 1B; PTPN2, T-cell protein-tyrosine phosphatase; PTGES, Prostaglandin E synthase; RMSD, Root mean square deviation; SOD, Serum total superoxide dismutase; SGPT, Serum glutamic-pyruvic transaminase; SGOT, serum glutamic-oxaloacetic transaminase; SGLT2, Sodium-glucose transport protein 2; STZ, Streptozotocin; SUR1, Sulfonylurea receptor; TC, Total cholesterol; TG, Triacylglycerol; T1D, Type 1 diabetes mellitus; T2D, Type 2 diabetes mellitus.

* Corresponding author.
E-mail address: aharrasi@unizwa.edu.om (A. Al-Harrasi).
[1] These authors equally contribute.

https://doi.org/10.1016/j.biopha.2022.112669
Received 14 November 2021; Received in revised form 20 January 2022; Accepted 24 January 2022
Available online 1 February 2022

2045, respectively. The prevalence in an urban area (10.8%) is higher than in the rural (7.2%) areas, and in high-income countries (10.4%) than low-income countries (4%) [1].

Natural products have gained great attention as a source of drug candidates globally and their use in drug discovery has increased to promote the traditional healthcare systems. About 80% of the world's population uses plant-based traditional health remedies due to their affordability and therapeutic safety [2]. Several species of *Boswellia* have shown interesting medicinal properties. The compounds *β*-BA and *β*-KBA (which belong to a group of pentacyclic triterpenoids) are solely isolated from the resins of *Boswellia* spp. with superior medicinal activities [3]. They inhibit growth and affect apoptosis in brain tumors, colon cancer cells, breast and prostate cancers cells, malignant glioma cells, and leukemia cells [4–7]. Moreover, their biological activities against ulcerative colitis, asthma, chronic colitis, hepatitis, inflammation, and arthritis are well documented [8–13]. They also act as chronic inflammatory agents, mainly by blocking the activities of 5-lipoxygenase and different cytokines (interleukins and TNF-α) [14–17]. *Boswellia* extract and *β*-KBA exert significant anti-diabetic potential by inhibiting the expression of proinflammatory cytokines from immune-competent cells and eventually prevent insulitis and insulin resistance in T1D and T2D, respectively. They can be considered as a promising therapy for the treatment of T1D and T2D [18–21].

Recently, we have reported boswellic acid derivatives as active inhibitors of α-glucosidase [3]. Considering the antidiabetic potential of boswellic acids, two main boswellic acids (*β*-BA and *β*-KBA) were isolated from *Boswellia sacra* in the current study and scrutinized in in vivo model of high-fat diet and low dose STZ-induced T2D with detailed parameters. Moreover, the inverse-docking approach was applied to predict the most appropriate physiological drug targets for *β*-BA and *β*-KBA. During the search for biological targets of these compounds, the Dipeptidyl peptidase 4 enzyme was identified as one of the potential binders of *β*-BA and *β*-KBA to exert their anti-diabetic activities. Dipeptidyl peptidase 4 (DPP-4, EC3.4.14.5) inhibitors are relatively new drugs used in T2D that significantly reduce blood glucose [22]. DPP-4 is a class of exopeptidase that selectively cleaves dipeptides at the N-terminal of different substrates including incretin hormones, neuropeptides, growth factors, and cytokines [23]. DPP-4 inhibitors (gliptins) were first introduced in 2006 for the oral treatment of T2D. The DPP-4 inhibitors increase the concentration of incretin glucagon-like peptide-1 (GLP-1) and gastric inhibitory polypeptide (GIP) hormones which in turn stimulate the secretion of insulin and inhibit the secretion of glucagon [24]. These two hormones stimulate insulin secretion under hyperglycemic conditions and contribute to ~70% of the post-prandial insulin secretion [25–27]. GLP-1 and GIP are peptide hormones with a short biological half-life due to rapid enzymatic degradation of these hormones by the DPP-4 enzyme [27–29]. Orally, small active molecules can be used to inhibit DPP-4. The administration of DPP-4 inhibitors leads to 2–3-folds elevation of endogenous GLP-1 concentration [30]. Other than GLP-1, DPP-4 has an indirect target" or "off-target" that also contributes to the normalization of glycemia in T2DM [31]. More, recently treatment of COVID 19 patients with DPP-4 inhibitors (sitagliptin) at the time of hospitalization was found to be associated with low mortality and improved clinical outcomes [32,33], thus making them useful agents for patients with COVID 19 and T2D. Several DPP-4 inhibitors including sitagliptin, saxagliptin, linagliptin, and alogliptin are approved by the FDA, whereas Vildagliptin has approval by the European Medicines Agency (EMA). However, these DPP-4 inhibitors have shown several side effects such as, upper respiratory tract and urinary tract infections, anaphylaxis, angioedema, nasopharyngitis, pancreatitis, headache, and arthralgia [34–36].

In this study, the antidiabetic potential of *β*-BA and *β*-KBA was studied initially in vivo model of high-fat diet and low dose STZ-induced T2D. Later, the antioxidant effects of *β*-BA and *β*-KBA were examined through total superoxide dismutase and malondialdehyde assays. Additionally, the anti-hyperlipidemic effects of *β*-BA and *β*-KBA were studied by examining the levels of total cholesterol, triacylglycerol, low-density lipoprotein cholesterol, and high-density lipoprotein cholesterol. While the mechanism of action of these compounds was predicted by *in-silico* inverse docking, which revealed that the anti-diabetic effects of the compounds are due to the inhibition of the DPP-4 enzyme. The complete mechanism of *β*-BA and *β*-KBA is shown in Fig. 1.

2. Experimental

2.1. Plant material and identification

The oleo-gum resins of *B. sacra* were collected from various locations of the Dhofar region (Sultanate of Oman) by a trustful partner (Mr. Saleh Al-Amri). The specimen (BSHR-01/2016) was deposited in the herbarium of the Natural and Medical Sciences Research Center (NMSRC).

2.2. Extraction and isolation

The air-dried ground material (1 kg) of *B. sacra* resin was exhaustively extracted with pure methanol at room temperature. The extract was dried by evaporating solvent through Rota vapor to yield methanol extract (820 g) which was subjected to column chromatography (SiO_2, 70–230 mesh; Merck, Munich, Germany) using a gradient solvent system of 10–60% n-hexane/EtOAc, then washed by pure EtOAc to get eight fractions (BSF1–BSF8). After taking TLC, three fractions $BSF_{5–7}$ (20–40% EtOAc/n-hexane) were combined and further subjected to column chromatography, using gradient solvent system of EtOAc/n-hexane to get a mixture of two compounds; *β*-BA and *β*-KBA, which were further purified by recycling chloroform HPLC and eluted as a UV-active (*β*-KBA) and UV-inactive (*β*-BA) at a retention time of 42 min with 4 ml/min flow rate. After in vitro study, both compounds (*β*-BA and *β*-KBA) were selected for further in vivo antidiabetic studies.

2.3. Chemicals

The ingredients of the high-fat diet such as casein sodium salt from bovine milk, cholesterol, sodium cholate sodium carboxymethylcellulose (Na-CMC), and DL-methionine were purchased from Sigma Aldrich. Vitamin and mineral complex were purchased from the local Pharmacy, whereas yeast powder and vegetable oils were procured from the local market.

Different organic solvents and chemicals used in extraction were purchased from local suppliers of Merck Germany. Streptozotocin (Sigma Aldrich), glibenclamide (Sanofi Aventis Pharma (Pvt) Ltd., Pakistan), and glucose estimation kits (S.D Chek Gold Germany) were used in this study. Other reagents used in this study were tween-80 (Scharlau Chem. Spain), normal saline (Utsoka Pharma (Pvt) Ltd Pakistan), biochemical reagents for lipid profile, LFTs Kits (Human Germany) and RFTs kit (Bioneed Germany diagnostic).

2.3.1. Animals

Adult Sprague Dawley rats in the weight range of 150–200 g were housed in the animal house of the Department of Pharmacy, University of Swabi, Khyber Pakhtunkhwa, Pakistan. The rats were divided into two dietary groups. One group was given a normal pellet diet (NPD) and the other groups were fed on a high-fat diet (HFD) (powdered NPD= 36.5 g, vegetable oils 31. g, casein 25 g, cholesterol 1 g, sodium cholate 0.5 g, vitamins and mineral complex 6 g, D-L methionine 0.3 g, yeast powder 0.1 g, sodium chloride 0.1 g) for two weeks. The animals were maintained at 12 h light and dark cycle at room temperature maintained at 22–25C in the animal house. All animal procedures were approved by the Departmental Animal Ethical Committee, University of Swabi, KPK, Pakistan (DAEC/PHARM/2016/15) and were conducted according to the UK animal scientific procedure act, 1986.

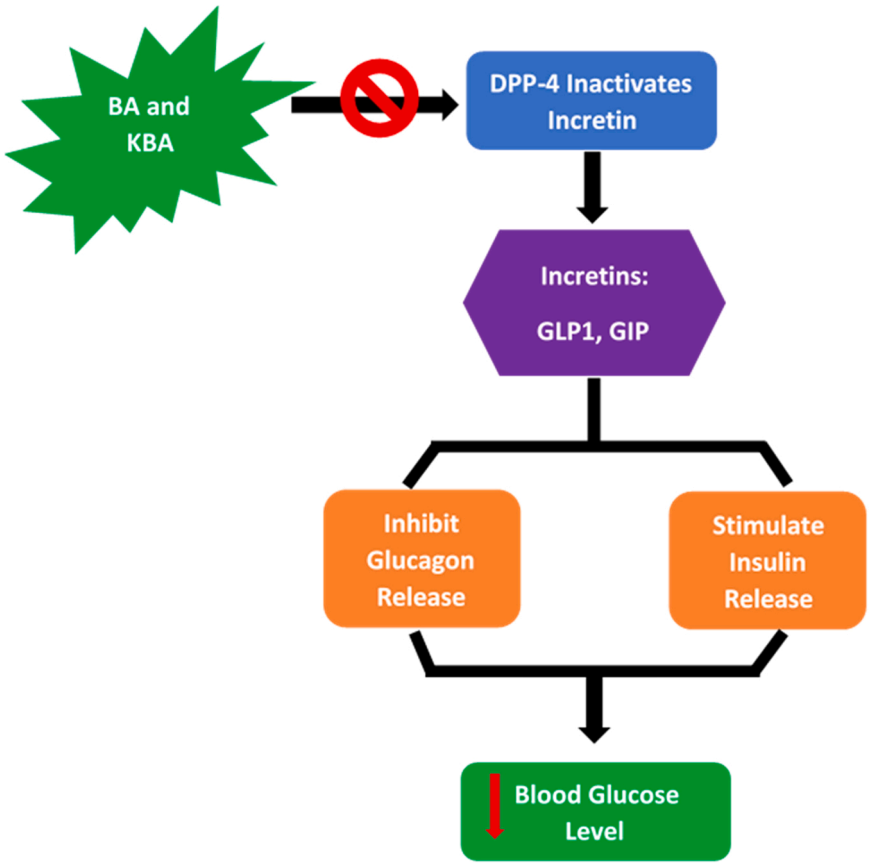

Fig. 1. The mechanism of β-BA and β-KBA. Both the compounds inhibit the DPP-4 enzyme in micromolar concentration. DPP-4 inactivates the incretin hormone which inhibits glucagon release and stimulates insulin release, thereby decreasing blood glucose level. β-BA and β-KBA increase the incretin by inhibiting DPP-4, thus decreasing the blood glucose level.

3. Biological assays

3.1. Examination of acute toxicity of β-BA and β-KBA

The acute toxicity of β-BA and β-KBA were determined by using adult Sprague Dawley rats weighing in the range of 160–200 g, according to the method described by Irwin (1968) [37]. The animals were divided into six groups (n = 6) for β-BA and β-KBA. Group 1 was used as a control which received 1% Tween 80 (vehicle) orally. Other groups (Group II- Group VI) received β-BA and β-KBA at a dose of 1, 2, 5, 10, and 20 mg/kg orally. Each animal was subjected to various parameters including writhing, convulsions, aggressiveness, hypersensitivity, salivation, lacrimation, spontaneous activity, ataxia, and catalepsy 30 min before injection (baseline) and then at 0 (straight after injection), 30 and 60 min, 24, 48 and 72 h and 1 week after administration. All the animals were observed for the same kind of behavioral, physical, and pharmacological toxic effects.

3.2. Induction of hyperglycemia

Hyperglycemia was induced in overnight fasting Sprague Dawley rats by a single intraperitoneal (i.p) injection of Streptozotocin (STZ, 50 mg/kg) reconstituted with ice-cold normal saline (0.9%). After 72 h of STZ injection, blood was collected from tail vein puncture with one-touch Glucometer strips using an SD glucometer (Germany) for estimation of glucose levels. Rats with fasting blood glucose levels> 300 mg/dl were considered diabetic and selected for the study.

3.3. Experimental design

All the animals were randomly divided into 9 groups (8 rats in each group). The first group served as normal control (non-diabetic) and received vehicle and NPD whereas the rest of the treatment groups were given HFD. The second group served as diabetic control and received STZ (50 mg/kg). The third group received a standard drug, glibenclamide (0.5 mg/kg, p.o). The fourth, fifth, and sixth groups were given β-BA orally at a dose of 1, 2 & 10 mg/kg, respectively. Whereas the seventh, eighth, and nine groups received β-KBA at a dose of 1, 2 & 10 mg/kg, respectively. The treatment was continued once daily at 09:00 am for 21 days. Bodyweight and blood glucose levels were estimated on the 1st, 5th, 8th, 10th, 15^{th,} and 21st day of treatment [38].

3.4. Estimation of biochemical parameters

After the completion of the antidiabetic assay on the 21st day, all animals were anesthetized with pentobarbital sodium (35 mg/kg) and euthanized by cervical decapitation using the method described in schedule 1 of the animal scientific procedure act 1986 and blood samples were collected through the cardiac puncture to study biochemical and oxidative parameters [39]. Collected blood was centrifuged at 1500g for 10 min for the separation of serum. The serum sample was then analyzed by a spectrophotometer (Perkin Elmer, Germany) for the determination of serum glutamic-pyruvic transaminase (SGPT), serum glutamic-oxaloacetic transaminase (SGOT), and serum alkaline phosphatase (ALP) using standard IFCC kinetic method (Bioneed kit Germany). Total cholesterol (TC), triglycerides (TG), low density lipoproteins (LDL), high-density lipoprotein (HDL), and serum creatinine were determined by CHOD-PAP [40]. Furthermore, C-peptide was

measured by Auto-analyzer or ELISA kits.

3.5. Antioxidant activity

3.5.1. Lipid peroxidation

Malondialdehyde (MDA) in serum was assayed by using a thiobarbituric acid (TBA) reactive substance at high temperature, thus resulting in the formation of a colored complex, which was expressed as nanomoles per milliliter plasma with a molar absorption coefficient of 156,000 $M^{-1}\cdot cm^{-1}$ at $\lambda = 532$ nm [41]. The reaction mixture consisted of 1 mM potassium permanganate, 10 mM phosphate buffer (pH 7.4), and the tested compounds. In the first step, 10 mM ferrous sulfate was added twice to initiate the reaction. Then, 20% trichloroacetic acid was added to stop the reaction process. Finally, malondialdehyde (MDA) reacted with thiobarbituric acid to form a colored product.

3.5.2. Superoxide dismutase

The serum superoxide dismutase (SOD) was determined following the previously described method [42] with modification. The absorbance of the reaction mixture was read at $\lambda = 540$ nm against the blank.

3.6. Histopathological assessment of liver, kidney, and pancreas

At the end of the study, after euthanasia, the liver, kidney, and pancreas tissues were fixed in 10% formalin solution for 48 h. The tissues were properly washed in running tap water, and dehydrated in descending grades of isopropanol and cleared in xylene. The tissues were then embedded in molten paraffin wax. Approximately 5 μm thick sections were prepared using a microtome and stained with Hematoxylin Eosin (H/E). The histopathological evaluation included 4–5 sections from each organ. Histopathological analysis of the liver, kidney, and pancreatic tissues was carried out under a light microscope 400X. Histological parameters were scored as described previously [43]. The visible histopathological features were graded and indicated as no change, mild, moderate and severe and were subsequently converted into numerical scoring consisting of Score 0 = no visible cell damage; Score 1 = damage < 30% of the tissue; score 2 = damage to 30–60% of the tissue; score 3 = Extensive necrosis involving damage to > 60% of the tissues.

4. Statistical analysis

All the values of blood glucose, body weight, and biochemical parameters were represented as mean ± S.E.M. Two groups were compared using Student's t-test, and more than two groups were compared by one way ANOVA followed by Dunnett's posthoc multiple comparison test. The non-parametric data based on scoring from histological studies were evaluated by the Kruskal-Wallis nonparametric analysis of variance (ANOVA) followed by the Dunns Posthoc test. Differences between groups were considered significant at $p < 0.05$.

4.1. In vitro inhibition of DPP-4 activity

The colorimetric assay against DPP-4 activity was based on a method described by Parmar et al. with slight modifications [44]. The assay was carried out by monitoring the DPP-4 mediated cleavage of the substrate GPPN to release p-nitroanilide, at 405 nm. Briefly, in a 96-well microplate, DPP-4 (150 U ml−1), dissolved in Tris-HCl (50 mM, pH 8.0), was pre-incubated at 37 ℃, for 10 min, with the tested samples (0–200 μM) dissolved in DMSO [final concentration of 9.1% (v/v)]. Subsequently, GPPN (0.25 mM), dissolved in Tris HCl (50 mM, pH 8.0), was added. Kinetic readings were initiated immediately after the addition of GPPN and maintained for 60 min, at 37 ℃. The enzymatic reaction was monitored using an ELISA plate reader (Spectra Max M2, Molecular Devices, CA, USA), by measuring the absorbance at 405 nm. The concentrations of DPP-4 and the tested samples refer to those attained before the addition of the substrate. The amount of DMSO used had no interference in the assay. The effects are expressed as the % inhibition of DPP-4 activity, calculated using the slope of the enzymatic reaction between 5 and 60 min. Sitagliptin (0–0.8 μM) was used as positive controls. The percent inhibition was calculated by using the following formula:

$$\% \text{ Inhibition} = 100\text{-(OD test well/OD control)} \times 100$$

5. Results and discussion

5.1. Isolation of β-BA and β-KBA

β-Boswellic acid was isolated as a white amorphous powder from the methanol extract of *B. sacra* resins. The molecular ion peak at *m/z* 455.3996 was determined by the high-resolution electrospray ionization mass spectrometry (HR-ESI-MS, Agilent 6530 LC Q-TOF (country of origin USA/EU, made in Singapore) corresponding to the loss of proton $[M—H]^+$, leading to the molecular formula $C_{30}H_{48}O_3$. The ^1H- and ^{13}C NMR spectra were recorded on nuclear magnetic resonance (NMR) spectrometer (Bruker, Zürich, Switzerland) operating at 600 MHz (150 MHz for ^{13}C) using the solvent peaks as internal references ($CDCl_3$, H: 7.26; C: 77.0). ^1H NMR spectra showed the presence of five tertiary methyls, two secondary methyls, and one double-bonded proton at δ_H 5.12 in the compound. The analysis of ^{13}C NMR data along with the distortionless enhancement by polarization transfer (DEPT) experiments and heteronuclear multiple quantum coherence (HMQC) correlations revealed the presence of seven methyls, nine methylenes, seven methines, and seven quaternary carbons, one carboxylic group at δ_C 183.16, two olefinic carbon atoms at δc 124.5 and 139.61. Based on the evidence given above and 2D NMR experiments using ^1H-^1H correlation spectroscopy (COSY), HMQC, and heteronuclear multiple bond coherence (HMBC) further confirmed the position of a double bond between C-12 and C-13 and carboxylic acid at C-24 poison, as a result, the structure was determined as *β*-BA (Fig. 2) [3,45].

Similarly, 11-keto-*β*-boswellic acid was isolated as white crystals from the methanol soluble extract of *B. sacra* resin. The mass spectrometry (HR-ESI-MS) exhibited a molecular ion peak at *m/z* 471.3473, $[M+H]^+$ corresponding to the molecular formula $C_{30}H_{47}O_4$ (calculated for $C_{30}H_{46}O_4$, 470.3396). ^1H NMR spectra displayed the presence of two secondary methyls, five tertiary methyls, and one double-bonded proton at δ_H 5.12. ^{13}C NMR data along with the DEPT experiments and 2D (HMQC and HMBC) correlations revealed the presence of 30 carbons including seven methyls, eight methylenes, seven methines, and eight quaternary carbons. Two olefinic carbon atoms at δc 131.3 and 167.61, one carbonyl group at δc 202.0, and one carboxylic group at δc 180.9 were determined by DEPT experiment. The position of these functional groups at C-12/13, C-11 and C-24 were further confirmed by 2D (HSQC, HMBC, and COSY) experiments) [3,45] and as a result, the structure was determined as *β*-KBA (Fig. 2).

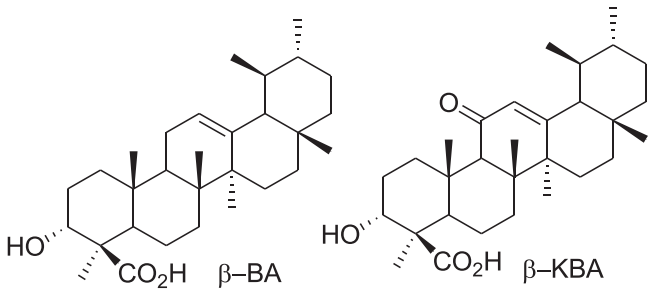

Fig. 2. The chemical structures of *β*-BA and *β*-KBA.

5.2. Acute toxicity of β-BA and β-KBA in STZ-induced diabetic rats

In the acute toxicity studies, the administration of β-BA and β-KBA was found safe at a dose level of 1, 2, 5, 10, and 20 mg/kg. The compounds did not produce any significant harmful changes in the behavior of the animals as observed by lack of convulsions, respiratory distress, writhing, changes to reflex activity, or mortality.

5.3. Antihyperglycemic effects of β-BA and β-KBA. in STZ-induced diabetic rats

The effects of β-BA, β-KBA, and glibenclamide on serum glucose levels in STZ induced diabetic rats are shown in Table 1. The standard reference drug, glibenclamide (0.5 mg/kg, p.o.) significantly reduced fasting blood glucose levels on day 5th, 7th, 10th, 15^{th,} and 21st day as compared to the diabetic control group as shown in Table 1. Chronic administration of β-BA at a dose of 1, 2, and 10 mg/kg also produced a significant antihyperglycemic effect on the 5th day onward in STZ-induced diabetic rats and significantly lowered the blood glucose level. The mean blood glucose level was reduced from 254 ± 25–137 ± 18 mg/dl at the highest dose tested (10 mg/kg). Similarly, the oral administration of β-KBA at a dose of 1, 2, and 10 mg/kg also produced a significant reduction in blood glucose level as shown in Table 1. Thus β-BA and β-KBA demonstrated good antihyperglycemic activity and did not cause any hypoglycemic effect unlike insulin and other synthetic drugs [46].

5.4. Effect of β-BA and β-KBA on Body Weight in STZ-induced diabetic rats

In diabetic control (untreated) rats, continued weight loss was observed till the end of the study (21 days treatment). During this period, a significant reduction in their body weight was recorded. However, STZ mediated bodyweight reduction was reversed by β-BA and β-KBA at the dose level of 1, 2, and 10 mg/kg and caused an improvement in body weight significantly (Table 2). This improvement in body weight was compared to that of glibenclamide-treated rats. This reversal of body weight loss can be attributed to the hypoglycemic effect of β-BA and β-KBA.

5.5. Effects of β-BA and β-KBA on biochemical in STZ-induced diabetic rats

The lipid profiles, the activity of hepatic marker enzymes, and renal function in serum in control and experimental rats are depicted in Table 3. In STZ-induced diabetic control rats, significant (**p<0.01, n = 8; Student's t-test) increase in total cholesterol (TC), TG, LDL cholesterol, and serum creatinine and a significant decrease (*p<0.05, n = 8; Student's t-test) in HDL cholesterol was observed as compared to the normal control. Whereas the administration of β-BA and β-KBA (at the dose of 1, 2, & 10 mg/kg, given for 21 days) showed a significant (**p<0.01, ***p<0.001, n = 8; one way ANOVA with Dunnett's posthoc test) reduction in TC, TGs and LDL cholesterol and dose-dependent increase of HDL cholesterol level as compared to the diabetic control rats. Furthermore, β-BA and β-KBA (1, 2 & 10 mg/kg) significantly reduced the serum SGPT, SGOT, ALP, and serum creatinine in rats intoxicated with STZ (**p<0.01, ***p<0.001, n = 8; one way ANOVA with Dunnett's posthoc test). Studies have shown that liver cells are destroyed irreversibly by STZ which increases the levels of different enzymes including SGPT, SGOT, and serum ALP in the blood [47]. In this study, β-BA and β-KBA significantly reduced the activities of these enzymes. This indicates the protective effects of β-BA and β-KBA on hepatocytes. Chronic hyperglycemia can also cause nephropathy that increases serum creatinine [48]. The reduction of serum creatinine by these compounds in treated rats may be due to the lowering of blood glucose levels. Furthermore, there was a slight decrease in c- peptide in the STZ-induced diabetic control group; however, it was statistically not significant when compared to the normal control and compounds treated groups (p > 0.05; n = 6) (Table 4).

5.6. Antioxidant activity of β-BA and β-KBA

Increasing evidence suggests the involvement of oxidative stress in hyperglycemia, impaired glucose tolerance, and diabetic complications. Oxidative stress is also implicated in beta-cell dysfunction and insulin resistance [49,50]. Furthermore, lipid peroxidation alters the antioxidant defense mechanism of the body leading to further impairment in glucose metabolism, extensive membrane damage, and dysfunction [51]. Thus, plasma malondialdehyde (MDA) serves as a useful marker of oxidative stress in pathological processes [52]. Serum total superoxide dismutase (SOD) IS one of the main antioxidant enzymes which maintains the cellular levels of oxygen within the physiological concentrations by converting superoxide anion radicals produced in the body to hydrogen peroxide [53]. Thus, SOD activity is a measure of the reactive oxygen species' elimination ability of the body indirectly. In the present study, compared with normal rats, MDA levels in diabetic control rats were significantly increased, whereas SOD activity was significantly decreased at the end of the treatment period. Oral administration of β-BA and β-KBA at the dose of 2 and 10 mg/kg, significantly decreased serum MDA level (p<0.05, 0.01), and increased serum SOD levels (p<0.05, 0.01) as compared to the diabetic control group. The standard reference drug glibenclamide also caused a significant decrease in serum MDA level and enhanced serum SOD levels indicating antioxidant effect (Table 4).

6. Histopathological analysis

6.1. Effect on liver

Fig. 3 shows the histopathological analysis of liver tissues and their description in Table 6 after the treatment period. Fig. 3A shows that liver architecture is normal in control animals. Liver sections in these animals

Table 1
Effect of daily oral administration of β-BA, β-KBA, and Glibenclamide on blood glucose level of STZ-induced diabetic rats.

S. No	Groups	Dose (mg/kg)	1st day	5th day	8th day	10th day	15th day	21st day
1	Normal control	**0.4 ml**	106 ± 8	110 ± 5	108 ± 6	105 ± 4	112 ± 3	108 ± 6
2	Diabetic control	**0.4 ml**	251 ± 20	274 ± 18	290.87 ± 20	316 ± 14	336 ± 30	354 ± 21
3	Glibenclamide	**0.5**	265 ± 11	213 ± 23*	180 ± 15* *	171 ± 12* *	152 ± 11* **	126 ± 10* **
4	β-BA	**1**	231 ± 13	223 ± 14 *	210 ± 17 *	190 ± 16 *	169 ± 12 *	150 ± 32 *
5	β-BA	**2**	240 ± 20	216 ± 12 *	205 ± 14 *	180 ± 11 *	164 ± 10 * *	145 ± 12 * *
6	β-BA	**10**	254 ± 25	210 ± 15 *	210 ± 19 *	167 ± 18 * *	150 ± 14 * *	137 ± 18 * **
7	β-KBA	**1**	264 ± 11	218 ± 10 *	205 ± 13 *	185 ± 10 *	160 ± 11 * *	155 ± 12 * *
8	β-KBA	**2**	248 ± 10	210 ± 12 *	200 ± 11 *	176 ± 10 * *	168 ± 9 * *	148 ± 12 * *
9	β-KBA	**10**	245 ± 24	209 ± 5 *	201 ± 98 *	163 ± 45 * *	164 ± 24 * *	136 ± 34 * **

The values are expressed as mean ± SEM. (n = 8 in each group). *P< 0.05, * *P< 0.01, * **P< 0.001 as compared with diabetic control at the same time (one-way ANOVA followed by Dunnett's multiple comparison test).

Table 2
Effects of β-BA and β-KBA on percentage bodyweight (B.W)t in STZ-induced diabetic rats.

Groups	Dose (mg/kg)	B.W on 1st Day	B.W (g) on 5th day	B.W (g) on 8th day	B.W (g) on 10th day	B.W (g) on 15th day	B.W (g) on 21st day
Normal control	**0.4 ml**	178 ± 22	168 ± 31	158 ± 45	154 ± 45	140 ± 19	125 ± 78
Diabetic control	**0.4 ml**	152 ± 7	157 ± 4 * **	161 ± 45	165 ± 32	169 ± 22	175 ± 82
Glibenclamide	**0.5**	153 ± 4	170 ± 5 * *	178 ± 43 * *	187 ± 67 * *	192 ± 23 * *	200 ± 45 * *
β-BA	**1**	162 ± 3	176 ± 4 * *	180 ± 22 * *	182 ± 78 * *	196 ± 33 * *	203 ± 04 * *
β-BA	**2**	163 ± 4	167 ± 6 * *	170 ± 34 * *	172 ± 28 * *	186 ± 13 * *	200 ± 23 * *
β-BA	**10**	161 ± 4	168 ± 9 * *	172 ± 23 * *	177 ± 39 * *	183 ± 21 * *	198 ± 34 * *
β-KBA	**1**	149 ± 9	167 ± 8 * *	170 ± 18 * *	172 ± 24 * *	179 ± 41 * *	199 ± 27 * *
β-KBA	**2**	156 ± 53	169 ± 2 * *	173 ± 29 * *	177 ± 35 * *	188 ± 24 * *	197 ± 28 * *
β-KBA	**10**	152 ± 43	172 ± 42 * *	175 ± 32 * *	187 ± 98 * *	196 ± 20 * *	207 ± 39 * *

The values are expressed as mean ± SEM. Each value corresponds to a mean of 8 animals. *p<0. 05, * *p<0.01; comparison of (diabetic control) vs (Glibenclamide, and β-BA and β-KBA treated groups) (One way ANOVA followed by posthoc Dunnett's multiple comparison test).

Table 3
The Effect of β-BA and β-KBA on biochemical parameters in STZ-induced diabetic rats.

Groups	Dose (mg/kg)	TC (mg/dl)	TG (mg/dl)	HDL (mg/dl)	LDL (mg/dl)	SGPT (IU)	SGOT (IU)	ALP (IU)	Serum Creatinine (mg/dl)
Normal Control	0.4 ml	203 ± 6.10	324 ± 7.40	15 ± 2.1	279 ± 3.5	214 ± 3.4	217 ± 4.5	372 ± 18.5	1.54 ± 0.3
Diabetic Control	0.4 ml	235.3 ± 3.4 * *	267.0 ± 6.9 * *	19.2 ± 2.2 *	265.4 ± 7.9	171.2 ± 11.8	243.4 ± 42.1 * *	293.8 ± 17.3 * *	2.4 ± 0.3 * *
Glibenclamide	0.5	136.7 ± 5.3 * *	127.3 ± 6.5 * *	48.1 ± 2.5 * *	87.3 ± 4.5 * **	38.5 ± 3.5 * *	18.5 ± 2.5 * *	126.9 ± 4.3 * *	0.6 ± 0.1 * **
β-BA	1	142.2 ± 4.3 * *	139.5 ± 5.7 * *	34.5 ± 2.1 * *	52.6 ± 2.2 * **	23.4 ± 8.0 * *	22.9 ± 3.9 * *	201.2 ± 17.55 * *	0.8 ± 0.1 * **
β-BA	2	152.5 ± 7.5 * *	134.8 ± 5.5 * *	45.6 ± 4.5 * *	41.5 ± 3.6 * **	21.4 ± 10 * *	21.7 ± 4.9 * *	191.2 ± 16.52 * *	0.7 ± 0.2 * **
β-BA	10	132 ± 3.2 * *	134.8 ± 5.5 * *	35.6 ± 4.5 * *	91.5 ± 3.6 * **	29.4 ± 10 * *	26.8 ± 4.9 * *	189.2 ± 15.21 * *	0.6 ± 0.2 * **
β-KBA	1	152.2 ± 4.3 * *	143.5 ± 5.7 * *	36.5 ± 1.1 * *	90.6 ± 2.2 * **	23.5 ± 8.0 * *	34.8 ± 3.9 * *	201.2 ± 16.55 * *	0.5 ± 0.1 * **
β-KBA	2	151.5 ± 7.5 * *	127.8 ± 5.5 * *	34.6 ± 3.5 * *	89.5 ± 3.6 * **	22.4 ± 10 * *	21.7 ± 4.9 * *	181.2 ± 17.22 * *	0.7 ± 0.2 * **
β-KBA	10	167.2 ± 2.4 * *	169.8 ± 2.7 * *	34.6 ± 3.5 * *	76.3 ± 7.2 * **	28.8 ± 28 * *	34.2 ± 3.2 * *	162.0 ± 19.56 * *	0.9 ± 0.5 * **

Each value is mean ± SEM of 8 animals. Comparisons were made between a normal control to diabetic control using student t-test (*p < 0.05, **p < 0.01) and between diabetic control to Glibenclamide/ β-BA and β-KBA) treated groups using one way ANOVA followed by Dunnett's posthoc multiple comparison test (** p < 0.01, ***p < 0.001).

Table 4
Effect of β-BA, β-KBA on serum MDA, SOD and c-peptide.

Groups	Dose (mg/kg)	MDA (nmol/ml)	SOD U/ml	c-peptide ng/ml
Normal Control	0.4 ml	2.60 ± 0.09	260.5 ± 8.5	0.09 ± 0.02
Diabetic Control	0.4 ml	7.12 ± 0.05 * **	180.4 ± 6.4 * *	0.06 ± 0.02
Glibenclamide	0.5	3.20 ± 0.09 * **	240.6 ± 7.8 * **	0.08 ± 0.01
β-BA	1	6.25 ± 0.05	255.5 ± 5.4	0.07 ± 0.02
β-BA	2	5.45 ± 0.07 *	220.2 ± 5.2 *	0.08 ± 0.01
β-BA	10	3.75 ± 0.06 * **	230.5 ± 7.3 * *	0.09 ± 0.01
β-KBA	1	5.95 ± 0.04	250.4 ± 6.8	0.06 ± 0.02
β-KBA	2	4.98 ± 0.06 * *	215.3 ± 6.5 *	0.07 ± 0.02
β-KBA	10	3.50 ± 0.08 * **	245.6 ± 4.8 * *	0.08 ± 0.01

Each value is mean ± SEM of 8 animals. Comparisons were made between normal control to diabetic control using student t-test (***p < 0.001) and between diabetic control to Glibenclamide β-BA and β-KBA) treated groups using one way ANOVA followed by Dunnett's posthoc multiple comparison test ((*p < 0.05, ** p < 0.01, ***p < 0.001).

showed unremarkable lines, parenchyma comprised of portal triads, central vein, and hepatocytes are arranged in cord fashion separated by sinusoidal spaces. STZ-induced diabetic animals showed severe patchy hemorrhagic necrosis of hepatocytes and periportal inflammation accompanied by dilation in sinusoidal spaces and lymphocytic infiltration (Fig. 3B). Glibenclamide treated group showed normal hepatocytes with portal vein and portal artery and showed only mild inflammation (Fig. 3C). Animals treated with the β-BA and β-KBA at the dose of 10 mg/kg showed protective effects in STZ-induced liver injury and showed only mild inflammation and almost normal hepatocytes (Figs. 3D and 3E). These results indicate the protective effects of β-BA and β-KBA on liver tissues.

6.2. Effect on kidney

Fig. 4 shows the histopathological effects on kidney tissues following treatment with β-BA and β-KBA and their description is given in Table 6. The results showed normal morphological features of the kidney such as prominent glomeruli, tubules, ascending and descending loops, and collecting ducts in the control group. STZ-induced diabetic animals showed the presence of crystal deposition on the glomeruli accompanied by severe infiltration of red blood cells and destructed glomeruli. Groups treated with glibenclamide, β-BA and β-KBA demonstrated the reversal of these pathological alterations as obvious from the regeneration of cells and removal of crystal deposition.

6.3. Effect on pancreas

Fig. 5 shows the histopathological changes following various treatments. The animals in the control group exhibited normal histological architecture. There were numerous rounded normal proportions of the islet of Langerhans which were present all around the pancreatic acini. Prominent nuclei with well-arranged lobules together with surrounding islets were found in the normal control rats. The STZ-induced diabetic group showedsevere cellular damage to the pancreatic acini and islets, which resulted in pancreatic β-cell damage followed by degeneration with asymmetrical vacuoles. The groups treated with glibenclamide, β-BA, and β-KBA showed reversal of these pathological changes and demonstrated marked improvement in the cellular damage caused by STZ. This improvement was evident from the more symmetrical vacuoles, partial restoration of islet cells, reduced β-cell damage, and increase in the number of islet cells. The description of these changes is given in Table 6.

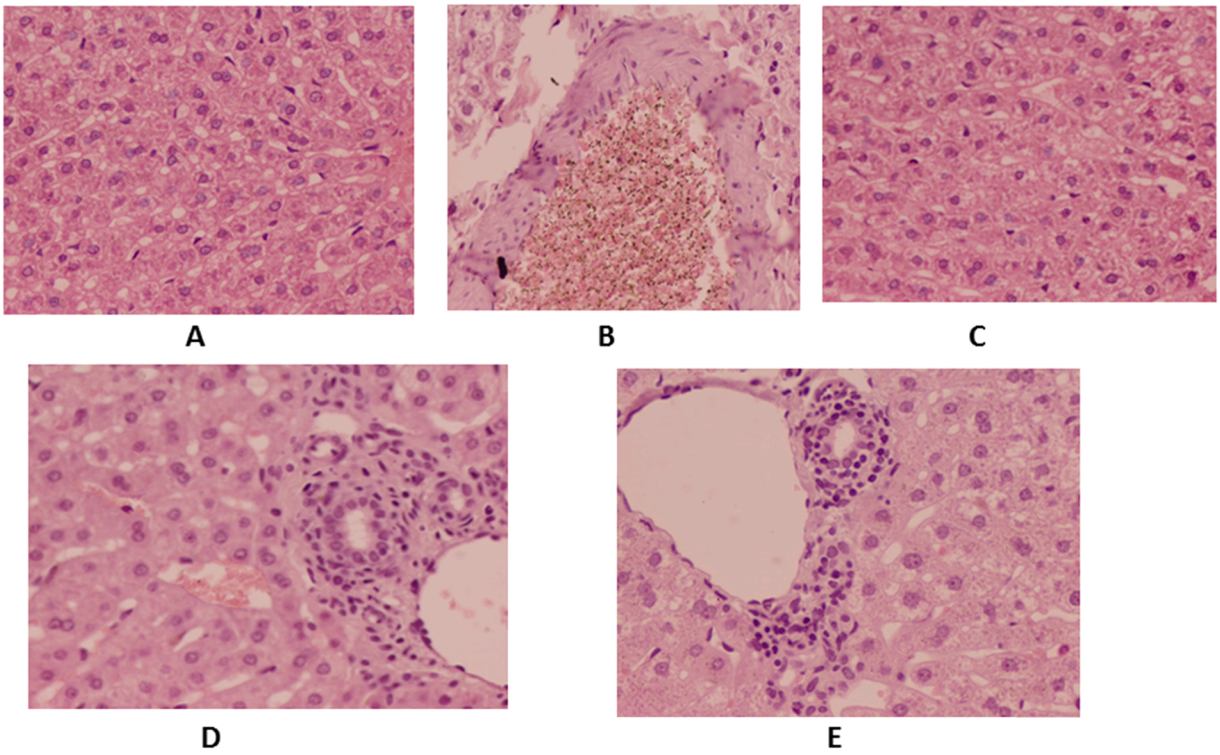

Fig. 3. Effect of β-BA and β-KBA on liver architecture in STZ-induced hepatic damage (A) Normal control group (B) STZ-induced diabetic group showing significant degenerative changes liver as compared to the normal control (**p<0.01). (C) glibenclamide (0.5 mg/kg) treated (D) β-BA 10 mg/kg (E) β-KBA 10 mg/kg. The histopathological changes in the liver are significantly reversed in glibenclamide, β-BA and β-KBA treated groups as compared to the STZ-induced diabetic group (**p<0.01).

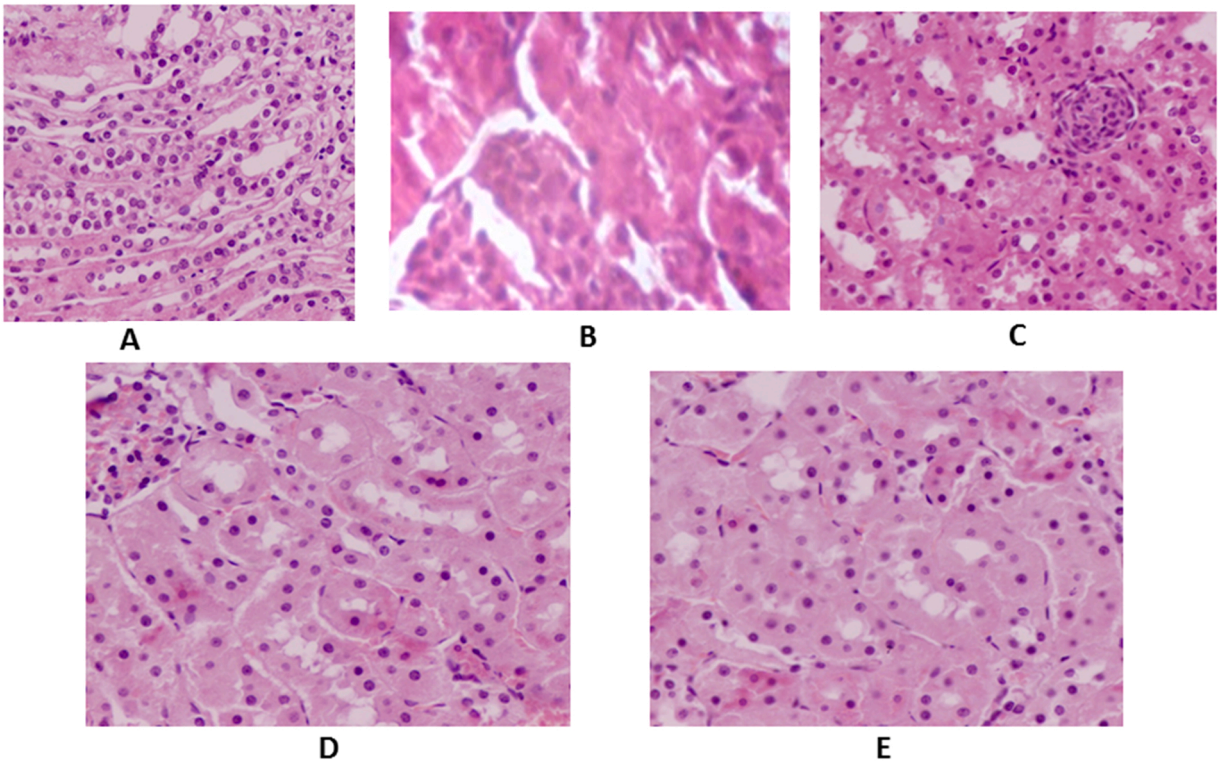

Fig. 4. Effect of β-BA and β-KBA on kidney in various groups of rats: (A) Normal control; there is the normal size of the glomerulus and cells shape (B) STZ-induced diabetic control; shows the presence of inflammatory cells in blood vessels and increase deposition of fats. STZ induced diabetic rats showed significant alterations in kidney architecture as compared to the normal control (**p<0.01). (C) glibenclamide (05 mg/kg) (D) β-BA 10 mg/kg (**E**) β-KBA 10 mg/kg. The histopathological changes in the kidney are partially reversed in glibenclamide, β-BA and β-KBA treated groups and were significant as compared to the STZ-induced diabetic group (**p<0.01).

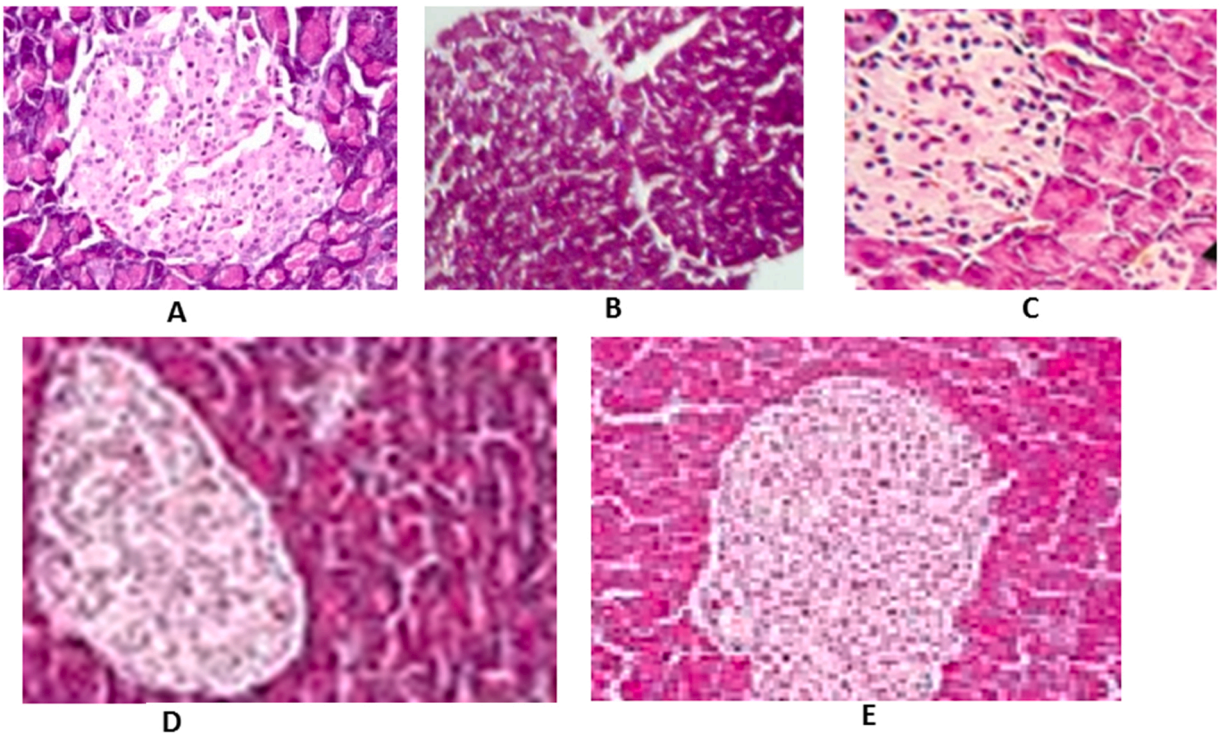

Fig. 5. Effect of β-BA and β-KBA on Histological changes of different control and treatment groups (A) Normal control group showing peripheral β-cell-rich area with an organized cellular mass of islet of the Langerhans (B) STZ-induced diabetic group showing the degenerative change in pancreatic architecture. STZ induced diabetic rats showed significant impairment in pancreatic architecture as compared to the normal control (***p<0.001). (C) glibenclamide (0.5 mg/kg) treated (D) *β*-BA 10 mg/kg (**E**) *β*-KBA 10 mg/kg. The histopathological changes in pancreatic tissues are reversed in glibenclamide, *β*-BA and *β*-KBA treated groups and were significant as compared to the STZ-induced diabetic group (**p<0.01).

6.4. In silico target fishing and inverse docking

The potential therapeutic biological targets of *β*-BA and *β*-KBA were predicted by both cheminformatics and structural bioinformatics approaches. Initially, a set of antidiabetics (Fig. S1) was selected from KEGG antidiabetic pathway (map07051) [54] (https://www.kegg.jp/). We identified nine biological targets that are specifically targeted by anti-diabetic drugs (currently present in the market). The anti-diabetic drugs are categorized as (i) Agonist of Insulin receptors (InsR), Peroxisome proliferator-activated receptor gamma (PPAR-γ), Glucagon-like peptide-1 receptor (GLP1), Free fatty acid receptor 1/Gprotein-coupled receptor (GPR40), and Sulfonylurea receptor agonists/ATP sensitive potassium channel (SUR1/Kir6.2) blockers, (ii) Inhibitors of Dipeptidyl peptidase 4 (DPP-4) enzyme, α-glucosidase enzyme and Sodium-glucose transport protein 2 (SGLT2) and (iii) Activators of 5' adenosine monophosphate-activated protein kinase (AMPK). Later, more biological targets of these compounds were explored by SwissTargetPrediction server [55] (www.swisstargetprediction.ch/), which showed that Prolyl endopeptidase (PREP), Prostaglandin E synthase (PTGES), Protein-tyrosine phosphatase 1B (PTP-1B), T-cell protein-tyrosine phosphatase (TC-PTP or PTPN2), Arachidonate 5-Lipoxygenase (ALOX5), and PPAR-γ are suitable drug target of *β*-BA, while ALOX5, PTP-1B, TC-PTP, and PTGES are probable drug targets for *β*-KBA (Table S1 and S2). Additionally, these compounds were searched on ChEMBL [56] (https://www.ebi.ac.uk/chembl/) database which revealed that both compounds possess weak activity against PREP, TC-PTP, PTGES, Cyclooxygenase-2, and PTP-1B. Moreover, *β*-BA also exhibits very low potency against DNA-(apurinic or apyrimidinic site) lyase, while *β*-KBA has shown lower potency against 11-beta-hydroxysteroid dehydrogenase 1 and 2, ALOX5. ChEMBL results agreed with the results of SwissTargetPrediction. Among the targets predicted by SwissTargetPrediction and ChEMBL, PTP-1B is a promising therapeutic diabetic drug target in type II diabetes mellitus (T2D). Based on these findings and extensive literature review, we selected nine potential physiological targets for *β*-BA and *β*-KBA, including Insulin receptor, PPAR-γ, GLP1, GPR40, SUR1/Kir6.2, DPP-4, α-glucosidase, AMPK, and PTP-1B. The structure of SGLT2 is not yet solved by X-ray crystallography or Nuclear Magnetic Resonance and is not deposited in the repository of protein databank, thus it was omitted in this study. The list of selected targets for *β*-BA and *β*-KBA is tabulated in Table S3.

Inverse structure-based docking was performed on the three-dimensional (3D-) structures of selected targets using Molecular Operating Environment (MOE version 2014.09). The 3D structure of each suggested target was downloaded from Protein Data Bank (rcsb.org) in complex with a ligand which may be an agonist or an inhibitor. Hydrogen atoms were added to all the structures to fulfill their valency. Protein-ligand interacting water molecules were retained, while the rest were removed from each PDB file. Partial charges were calculated based on MMFF-94x forcefield. Active site or ligand binding site was defined by using the bound ligand present in the PDB files of all targets. In insulin receptors, insulin binding residues were targeted. Two-dimensional structures of *β*-BA and *β*-KBA were drawn on ChemDraw and converted into 3D by MOE. Protons were added on both the structures and partial charges were calculated by MMFF-94x force field. The compound's structures were energy minimized till the RMS gradient of 0.1RMS kcal/mol/Å was achieved. For docking, the Triangle Matcher docking method was used in combination with the London dG scoring function and Force field refinement method. Thirty docked conformations of both compounds were retained as a default parameter, however, based on the compound's flexibility, a different number of docked conformations were generated by MOE on each biological target. Later, based on the docking scores and binding interactions of ligands with the selected biological target, the most appropriated docked conformation was selected by conformational sampling.

6.5. Computational prediction of probable drug targets of β-BA and β-KBA

Structure-based bioinformatic approaches play a significant role in the prediction of a specific biological target for any compound. We applied both cheminformatics and bioinformatics approaches to predict the most appropriate physiological targets of β-BA and β-KBA. The anti-diabetic drugs pathway was studied from the KEGG database, which showed that most of the anti-diabetic drugs act as an agonist of the insulin receptor, sulfonylurea receptor, GLP-1 receptor, GPR-40, and PPAR-γ, while some of the drugs inhibit the activity of α-glucosidase, DPP-4, and SGLT2. Moreover, other drugs block ATP-sensitive potassium channels (SUR1/Kir6.2). While metformin and buformin are the drugs that activate the enzyme AMPK. Additionally, we explored various drug targets from SwissTargetPrediction and ChEMBL, which suggested that Protein-tyrosine phosphatase 1B (PTP-1B) could be a probable drug target of these compounds. Thus, an inverse docking approach was applied to predict the binding potential β-BA and β-KBA towards those probable drug targets.

To test the docking accuracy of MOE, initially, re-docking was performed. The bound ligands were extracted from each protein (except InsR) and re-docked at their cognate space in their 3D structure. The performance of Redocking was scrutinized by calculating the root mean square deviation (RMSD) between the docked conformation and the native X-ray conformation of the ligand. Re-docking results were promising, and all the compounds were docked with RMSD $\leq$ 3.0 Å (Table S4). This criterion suggests that the docking method can find docked orientation close to the experimentally determined conformation in the X-ray structure. Thus, the applied docking method is robust enough to be used in inverse docking protocol. The superimposed view of docked conformation and the reference conformation of compounds are shown in Fig. S2.

Inverse docking results showed that the binding preference of β-BA and β-KBA towards DPP-4 and α-Gluc is high, followed by Sur1/Kir6.2. On these targets, both the compounds exhibited docking scores (DS) in the range of > -9. While the DS of β-BA and β-KBA in the binding pockets of InsR, PPAR-γ, GLP-1, AMPK, and PTP-1 was in the range of < -9 to > -6. Based on DS, DPP-4 (DS=−9.59 Kcal/mol), α-Gluc (DS = −9.20Kcal/mol) and SUR1/Kir6.2 (−9.05) were retrieved as potential targets for β-BA. Whereas β-BA exhibited moderate binding affinities for GLP1 (−8.99), InsR (−8.45), PPAR-γ (−8.37), and PTP1B (DS = −8.03), and least affinity for AMPK (DS = −6.99). Similarly, the DS of β-KBA on DPP-4 (−10.90), α-Gluc (DS = −9.29), and SUR1/Kir6.2 (DS = −9.11) was high, while GLP-1 (DS = −8.69), InsR (DS = −8.33), and PTP1B (DS = −8.08) showed moderate to lower binding potential for β-KBA, whereas AMPK (DS = −7.47) and PPAR-γ (−7.04) were identified as least preferred binders. However, the DS of both the compounds on GPR40 reflects that these compounds could not inhibit GPR40 (DS of β-BA = +17.78 and β-KBA = +19.19) and the binding of these compounds with GPR40 is an unfavorable and an endothermic process (Table S5). The binding potential of β-BA and β-KBA for different targets is shown in Fig. 6. The binding interactions of both compounds on each selected target are being discussed in Supporting information.

6.6. Comparison of docking scores of β-BA and β-KBA with the reference ligands

β-BA and β-KBA exhibited higher DS as compared to reference compounds, Glibenclamide, Vildagliptin, Acarbose, and 97 V which are inhibitors of SUR1/Kir6.2, DPP-4, α-glucosidase, and agonist of GLP1, respectively. β-BA and β-KBA exhibited a comparable binding score with the PPAR-γ agonist. Both the compounds depicted lower binding affinities for AMPK, PTP-1B and GPR40 as compared to the AMPK activator (DS = −7.95), PTP-1B inhibitor (DS = −10.75) and GPR40 agonists (DS = −9.35), respectively. Based on the docking results, we predict that DPP-4, α-Gluc, and Sur1/Kir6.2 could be the most potential physiological targets for β-BA and β-KBA (Table S5). The docking results of β-BA and β-KBA on different biological targets are discussed in Supporting information. The binding modes of β-BA and β-KBA in the ligand-binding sites of selected druggable proteins are shown in Figs. S3–S10.

6.7. Binding Interactions of β-BA and β-KBA with dipeptidyl peptidase 4

DPP-4 is involved in signal transduction, immune regulation, apoptosis, glucose metabolism, and regulates the degradation of incretins like Glucagon-like peptide-1 (GLP-1) which stimulates glucose-dependent insulin release from the pancreas. DDP-4 inhibitors reduce glucagon and blood glucose levels, thus can be used to treat T2DM. DPP-4 inhibitors can be given to patients with chronic kidney disease who are intolerant to metformin. Moreover, some DPP-4 inhibitors are linked with an increased risk of heart failure. Thus, safer DDP-4 inhibitors are required. In our inverse docking results, β-KBA (−10.90Kcal/mol) showed higher binding potential for DDP-4, while β-BA (−9.59Kcal/mol) also depicted good binding affinities with this enzyme. Moreover, both the compounds exhibited higher binding potential as compared to the reference drug Vildagliptin (DS= −7.28Kcal/mol). Vildagliptin binds with the active site residues Glu205, Glu206, Arg125, Asn710, Tyr631, and a water molecule through H-bonding while Glu206 also provides ionic interactions to the Vildagliptin. The docked orientation of β-KBA exposed that carboxylic group of the compound mediates H-bonding with the side chain of Glu206 and a water molecule. Moreover, Arg669 and a water molecule seem to donate H-bond to this group. While carbonyl moiety has a chance to interact with three water molecules in the vicinity, the -OH group can donate H-bond to the side chain of Tyr662. The water-mediated protein-ligand bridging are playing important role in the stabilization of β-KBA. The compound is neatly accommodated in the active site of DPP-4. β-BA also binds at the same position; however, its carboxylic group is tilted more towards Asn710 which provides bidentate interactions to the carboxylic group of β-BA. The -OH group of β-BA does not interact with the surrounding residues, while the lack of carbonyl group is responsible for the lack of water-mediated protein-ligand interactions. Because of this reason, β-BA showed less affinity towards DPP-4 as compared to β-KBA. The binding modes of β-BA and β-KBA are shown in Fig. 7.

Fig. 6. Binding potential of β-BA and β-KBA on the selected drug targets based on docking score. Green color indicates higher potential, low to least binding potential is depicted in orange to red color. (For interpretation of the references to colour in this figure, the reader is referred to the web version of this article.)

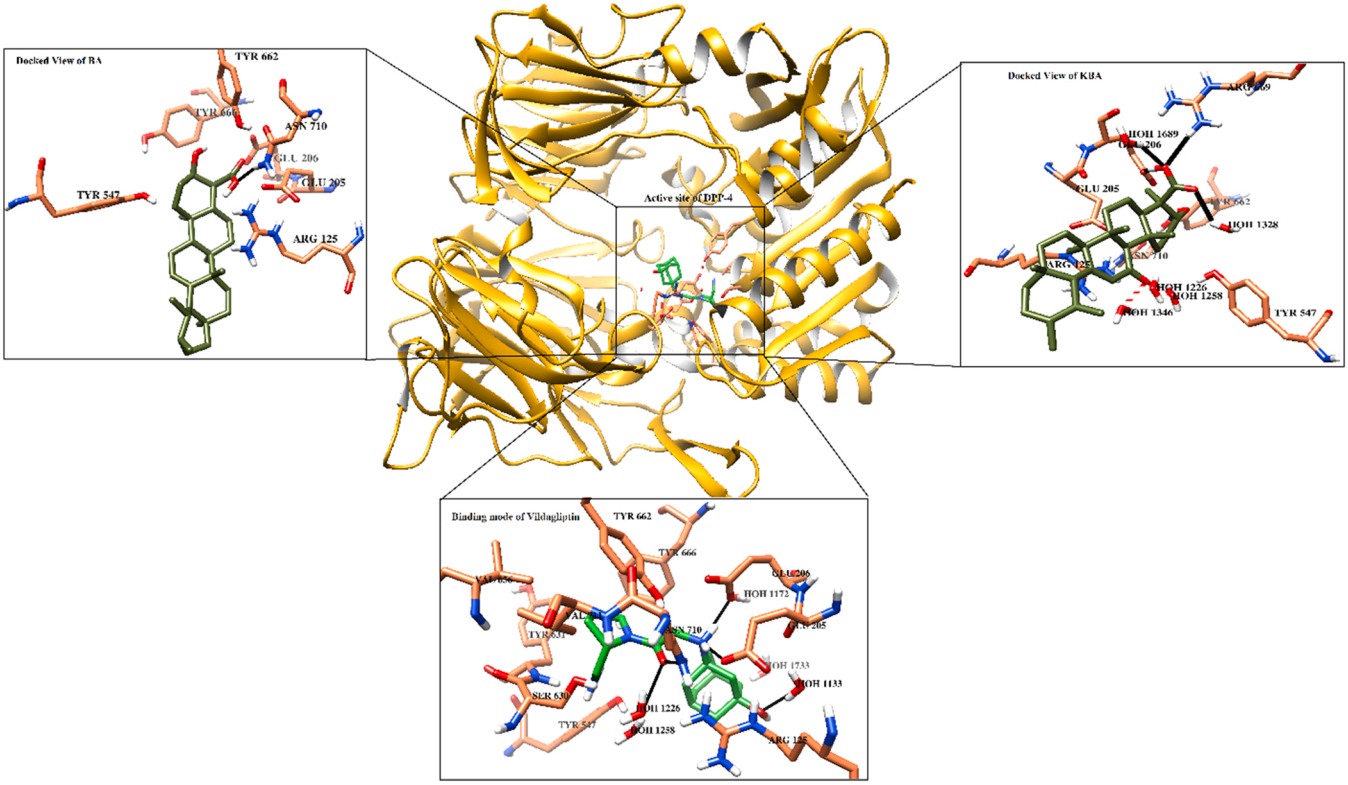

Fig. 7. The binding modes of *β*-BA and *β*-KBA are shown in the active site of DPP-4 (golden ribbon). The binding mode of Vildagliptin (lime green sticks) is highlighted in a box. *β*-BA and *β*-KBA are shown in the olive green stick model, interacting residues are depicted in the coral stick model, H-bonds are displayed in black lines, the chance of H-bonding in *β*-KBA is displayed in red dotted lines. (For interpretation of the references to colour in this figure, the reader is referred to the web version of this article.)

6.8. *In-vitro validation of DPP-4 activity of β-BA and β-KBA*

Based on the DS, DPP-4 was identified as the top-ranked biological target of *β*-BA and *β*-KBA. The *in-silico* findings were validated by testing the inhibitory potential on *β*-BA and *β*-KBA against the DPP-4 enzyme. In in-vitro testing, both *β*-BA and *β*-KBA possessed significant DPP-4 inhibition with IC_{50} values of 3.06 ± 0.85 and 1.65 ± 0.065 μM, respectively. *β*-KBA exhibited two-times better activity than *β*-BA (Table 5). The DS and binding interactions of *β*-KBA (−10.90 kcal/mol) was higher than the DS (−9.59 kcal/mol) and binding interaction of *β*-BA. Therefore our in vitro validation results complement our docking results completely. In our previous studies, α-glucosidase inhibitory potential of *β*-BA and *β*-KBA were scrutinized in-vitro on *Saccharomyces cerevisiae* α-glucosidase [3]. In in vitro test, *β*-BA showed weak inhibition of *S. cerevisiae* α-glucosidase while *β*-KBA exhibited significant inhibition with IC_{50} of 52.9 ± 4.66 μM. The current *in silico* study indicates that these compounds may show good inhibitory potential for human α-glucosidase.

Table 5
DPP-4 inhibitory activity of *β*-BA and *β*-KBA.

Compounds	Docking Score (kcal/mol)	% Inhibition	IC_{50} ± SEM (μM)
β-BA	-8.69	86.4	3.06 ± 0.85
β-KBA	-10.90	82.3	1.65 ± 0.065
Sitagliptin (standard)		92.8	0.106 ± 0.006

7. Conclusions

In conclusion, *β*-BA and *β*-KBA decreased the blood glucose level significantly in fasting STZ-induced diabetic rats caused a significant reduction in the lipid and lowered various biochemical parameters including SGPT, SGOT, ALP, and serum creatinine in diabetic rats. The lowering of blood glucose level and effects on the pancreatic β-cells of islets of Langerhans indicate a strong antidiabetic potential of *β*-BA and *β*-KBA. Moreover, the inverse docking method was applied to elucidate the molecular mechanism/s involved in the antidiabetic activity of *β*-BA and *β*-KBA. Our *in-silico* results indicate the antidiabetic effect observed in this study might be mediated via inhibition of DPP-4 and GLP1 and Insulin receptors can be potential biological targets for *β*-BA and *β*-KBA. Furthermore, *β*-BA and *β*-KBA and their analogs could provide useful leads for the development of novel therapeutics for treating patients with COVID 19 and T2D.

Ethics approval

All animal procedures were approved by the Departmental Animal Ethical Committee, University of Swabi, KPK, and Pakistan (DAEC/PHARM/2016/15) and were conducted according to the UK animal scientific procedure act, 1986.

Consent for publication

Not applicable.

Table 6
Histological injury score of liver, kidney, and pancreas after treatment for 21 days with glibenclamide, β-BA, and β-KBA.

Groups	Injury score							
	Liver			Kidney			Pancreas	
	Necrosis	Sinusoidal dilatation	Infiltration of inflammatory cells	Necrosis of tubular epithelial cells	Glomerular deformity	Infiltration of red blood cells	Pancreatic islets cell necrosis	Asymmetrical vacuolization
Normal control	0	0	0	0	0	0	0	0
Diabetic control	3	3	3	3	3	3	3	3
Glibenclamide (0.5 mg/kg)	1 * *	1 * *	2	1 * *	1 * *	2	1 * *	1 * *
β-BA(10 mg/kg)	1 * *	2	1 * *	1 * *	1 * *	1 * *	2	1 * *
β-KBA (10 mg/kg)	1 * *	1 * *	1 * *	1 * *	1 * *	2	1 * *	1 * *

Liver, kidneys and pancreas were scored for histopathological parameters via light microscopy with Score 0 = no visible cell damage; Score 1 = damage < 30% of the tissue; score 2 = damage to 30–60% of the tissue; score 3 = Extensive necrosis up to > 60% of the tissues. Data were analyzed by the Kruskal-Wallis nonparametric analysis of variance (ANOVA) followed by Dunns Posthoc test (**p<0.001; n = 6).

Funding

The project was supported by a grant from The Oman Research Council (TRC) through the funded project (BFP/RGP/HSS/19/198).

CRediT authorship contribution statement

AAH, and AK conceived and designed the study. NK, IK, NUR and MK performed all experiments. SAH and AK performed all computational studies and analyzed the data. WA and RC helped in the analysis of data. NK, SAH and AK wrote the manuscript with inputs and comments from all co-authors. All authors have read and approved the final version of the manuscript. All data were generated in-house, and no paper mill was used.

Conflict of interest statement

The authors declare that they have no known competing financial interests or personal relationships that could have appeared to influence the work reported in this paper.

Data Availability

No data was used for the research described in the article.

Acknowledgments

The authors would like to thank the University of Nizwa for the generous support of this project and the Oman Research Council (TRC) through the funded project (BFP/RGP/HSS/19/198). We thank the technical staff for their assistance. The authors are thankful to the Higher Education Commission of Pakistan for providing the Start-Up Research Grant 2017 (SRGP-1230) for financing this research from beginning till completion.

Appendix A. Supporting information

Supplementary data associated with this article can be found in the online version at doi:10.1016/j.biopha.2022.112669.

References

[1] P. Saeedi, I. Petersohn, P. Salpea, B. Malanda, S. Karuranga, N. Unwin, S. Colagiuri, L. Guariguata, A.A. Motala, K. Ogurtsova, Global and regional diabetes prevalence estimates for 2019 and projections for 2030 and 2045: results from the International Diabetes Federation Diabetes Atlas, Diabetes Res. Clin. Pract. 157 (2019), 107843.
[2] M. Maciel, A. Pinto, V. Veiga, N. Grynberg, A. Echevarria, Medicinal plants: the need for multidisciplinary scientific studies, Quím. Nova 25 (3) (2002) 429–438.
[3] N.U. Rehman, A. Khan, A. Al-Harrasi, H. Hussain, A. Wadood, M. Riaz, Z. Al-Abri, New α-Glucosidase inhibitors from the resins of Boswellia species with structure–glucosidase activity and molecular docking studies, Bioorg. Chem. 79 (2018) 27–33.
[4] G. Janssen, U. Bode, H. Breu, B. Dohrn, V. Engelbrecht, U. Göbel, Boswellic acids in the palliative therapy of children with progressive or relapsed brain tumors, Klin. Padiatr. 212 (04) (2000) 189–195.
[5] J.-J. Liu, Å. Nilsson, S. Oredsson, V. Badmaev, W.-Z. Zhao, R.-D. Duan, Boswellic acids trigger apoptosis via a pathway dependent on caspase-8 activation but independent on Fas/Fas ligand interaction in colon cancer HT-29 cells, Carcinogenesis 23 (12) (2002) 2087–2093.
[6] T. Glaser, S. Winter, P. Groscurth, H. Safayhi, E. Sailer, H. Ammon, M. Schabet, M. Weller, Boswellic acids and malignant glioma: induction of apoptosis but no modulation of drug sensitivity, Br. J. Cancer 80 (5) (1999) 756–765.
[7] R. Hoernlein, T. Orlikowsky, C. Zehrer, D. Niethammer, E. Sailer, T. Simmet, G. Dannecker, H. Ammon, Acetyl-11-keto-β-boswellic acid induces apoptosis in HL-60 and CCRF-CEM cells and inhibits topoisomerase I, J. Pharmacol. Exp. Ther. 288 (2) (1999) 613–619.
[8] I. Gupta, A. Parihar, P. Malhotra, G.B. Singh, R. Ludtke, H. Safayhi, H.P. Ammon, Effects of Boswellia serrata gum resin in patients with ulcerative colitis, Eur. J. Med Res 2 (1997) 37–43.
[9] S. Singh, A. Khajuria, S.C. Taneja, R.K. Khajuria, J. Singh, G.N. Qazi, Boswellic acids and glucosamine show synergistic effect in preclinical anti-inflammatory study in rats, Bioorg. Med. Chem. Lett. 17 (13) (2007) 3706–3711.
[10] I. Gupta, A. Parihar, P. Malhotra, S. Gupta, R. Lüdtke, H. Safayhi, H.P. Ammon, Effects of gum resin of Boswellia serrata in patients with chronic colitis, Planta Med. 67 (05) (2001) 391–395.
[11] H. Safayhi, T. Mack, H.T. Ammon, Protection by boswellic acids against galactosamine/endotoxin-induced hepatitis in mice, Biochem. Pharmacol. 41 (10) (1991) 1536–1537.
[12] L. Ali, J. Hussain, A. Al-Rawahi, A. Al-Harrasi, Two New and Four Known Triterpenoids from Boswellia sacra Fluckiger, Rec. Nat. Prod. 8 (4) (2014) 407.
[13] S. Shenvi, K. Kiran, K. Kumar, L. Diwakar, G.C. Reddy, Synthesis and biological evaluation of boswellic acid-NSAID hybrid molecules as anti-inflammatory and anti-arthritic agents, Eur. J. Med. Chem. 98 (2015) 170–178.
[14] H. Ammon, Boswellic acids in chronic inflammatory diseases, Planta Med. 72 (12) (2006) 1100–1116.
[15] N.C. Gilbert, J. Gerstmeier, E.E. Schexnaydre, F. Börner, U. Garscha, D.B. Neau, O. Werz, M.E. Newcomer, Structural and mechanistic insights into 5-lipoxygenase inhibition by natural products, Nat. Chem. Biol. 16 (7) (2020) 783–790.
[16] U. Siemoneit, C. Pergola, B. Jazzar, H. Northoff, C. Skarke, J. Jauch, O. Werz, On the interference of boswellic acids with 5-lipoxygenase: mechanistic studies in vitro and pharmacological relevance, Eur. J. Pharmacol. 606 (1–3) (2009) 246–254.
[17] D. Poeckel, L. Tausch, N. Kather, J. Jauch, O. Werz, Boswellic acids stimulate arachidonic acid release and 12-lipoxygenase activity in human platelets independent of Ca2+ and differentially interact with platelet-type 12-lipoxygenase, Mol. Pharmacol. 70 (3) (2006) 1071–1078.
[18] A.M. Shehata, L. Quintanilla-Fend, S. Bettio, Z. Kamyabi-Moghaddam, U. A. Kohlhofer, W.A. Scherbaum, H.P. Ammon, 11-keto-β-boswellic acid inhibits lymphocyte (CD3) infiltration into pancreatic islets of young none obese diabetic (NOD) mice, Horm. Metab. Res. 49 (09) (2017) 693–700.
[19] A. Shehata, L. Quintanilla-Fend, S. Bettio, J. Jauch, T. Scior, W. Scherbaum, H. Ammon, 11-Keto-β-boswellic acids prevent development of autoimmune reactions, insulitis and reduce hyperglycemia during induction of multiple low-dose streptozotocin (MLD-STZ) diabetes in mice, Horm. Metab. Res. 47 (06) (2015) 463–469.
[20] A.M. Shehata, L. Quintanilla-Fend, S. Bettio, C. Singh, H. Ammon, Prevention of multiple low-dose streptozotocin (MLD-STZ) diabetes in mice by an extract from gum resin of Boswellia serrata (BE), Phytomedicine 18 (12) (2011) 1037–1044.
[21] H. Ammon, Boswellic extracts and 11-keto-ß-boswellic acids prevent type 1 and type 2 diabetes mellitus by suppressing the expression of proinflammatory cytokines, Phytomedicine 63 (2019), 153002.
[22] K. Makrilakis, The role of DPP-4 inhibitors in the treatment algorithm of type 2 diabetes mellitus: when to select, what to expect, Int. J. Environ. Res. Public Health 16 (15) (2019) 2720.

[23] D. Röhrborn, N. Wronkowitz, J. Eckel, DPP4 in diabetes, Front. Immunol. 6 (2015) 386.
[24] B. Gallwitz, Clinical use of DPP-4 inhibitors, Front. Endocrinol. 10 (2019).
[25] W. Creutzfeldt, The incretin concept today, Diabetologia 16 (2) (1979) 75–85.
[26] M. Nauck, E. Bartels, C. Orskov, R. Ebert, W. Creutzfeldt, Additive insulinotropic effects of exogenous synthetic human gastric inhibitory polypeptide and glucagon-like peptide-1-(7-36) amide infused at near-physiological insulinotropic hormone and glucose concentrations, J. Clin. Endocrinol. Metab. 76 (4) (1993) 912–917.
[27] M.A. Nauck, J.J. Meier, Incretin hormones: their role in health and disease, Diabetes, Obes. Metab. 20 (2018) 5–21.
[28] D.J. Drucker, M.A. Nauck, The incretin system: glucagon-like peptide-1 receptor agonists and dipeptidyl peptidase-4 inhibitors in type 2 diabetes, Lancet 368 (9548) (2006) 1696–1705.
[29] R. Mentlein, B. Gallwitz, W.E. Schmidt, Dipeptidyl-peptidase IV hydrolyses gastric inhibitory polypeptide, glucagon-like peptide-1 (7–36) amide, peptide histidine methionine and is responsible for their degradation in human serum, Eur. J. Biochem. 214 (3) (1993) 829–835.
[30] J.J. Holst, C.F. Deacon, Inhibition of the activity of dipeptidyl-peptidase IV as a treatment for type 2 diabetes, Diabetes 47 (11) (1998) 1663–1670.
[31] C.F. Deacon, Physiology and pharmacology of DPP-4 in glucose homeostasis and the treatment of type 2 diabetes, Front. Endocrinol. 10 (2019) 80.
[32] S.B. Solerte, F. D'Addio, R. Trevisan, E. Lovati, A. Rossi, I. Pastore, M. Dell'Acqua, E. Ippolito, C. Scaranna, R. Bellante, S. Galliani, A.R. Dodesini, G. Lepore, F. Geni, R.M. Fiorina, E. Catena, A. Corsico, R. Colombo, M. Mirani, C. De Riva, S. E. Oleandri, R. Abdi, J.V. Bonventre, S. Rusconi, F. Folli, A. Di Sabatino, G. Zuccotti, M. Galli, P. Fiorina, Sitagliptin treatment at the time of hospitalization was associated with reduced mortality in patients with type 2 diabetes and COVID-19: a multicenter, case-control, retrospective, observational study, Diabetes Care 43 (12) (2020) 2999–3006.
[33] S.B. Solerte, A. Di Sabatino, M. Galli, P. Fiorina, Dipeptidyl peptidase-4 (DPP4) inhibition in COVID-19, Acta Diabetol. 57 (7) (2020) 779–783.
[34] R. Pathak, M.B. Bridgeman, Dipeptidyl peptidase-4 (DPP-4) inhibitors in the management of diabetes, Pharm. Ther. 35 (9) (2010) 509.
[35] T. Karagiannis, P. Boura, A. Tsapas, Safety of dipeptidyl peptidase 4 inhibitors: a perspective review, Ther. Adv. Drug Saf. 5 (3) (2014) 138–146.
[36] S. Montilla, G. Marchesini, A. Sammarco, M. Trotta, P. Siviero, C. Tomino, D. Melchiorri, L. Pani, AADM Group, Drug utilization, safety, and effectiveness of exenatide, sitagliptin, and vildagliptin for type 2 diabetes in the real world: data from the Italian AIFA Anti-diabetics Monitoring Registry, Nutr., Metab. Cardiovasc. Dis. 24 (12) (2014) 1346–1353.
[37] S. Irvin, comprehensive observational assessment: a systematic quantitative procedure for assess_ing the behavioral and physiologic state of the mouse, Phychopharmacologia 13 (3) (1968) 222–257.
[38] R. Gupta, K.G. Bajpai, S. Johri, A. Saxena, An overview of Indian novel traditional medicinal plants with anti-diabetic potentials, Afr. J. Tradit., Complement. Altern. Med. 5 (1) (2008) 1–17.
[39] A. Nagappa, P. Thakurdesai, N.V. Rao, J. Singh, Antidiabetic activity of Terminalia catappa Linn fruits, J. Ethnopharmacol. 88 (1) (2003) 45–50.
[40] M. Uchiyama, M. Mihara, Determination of malonaldehyde precursor in tissues by thiobarbituric acid test, Anal. Biochem. 86 (1) (1978) 271–278.
[41] B. Melekh, I. Ilkiv, A. Lozynskyi, A. Sklyarov, Antioxidant enzyme activity and lipid peroxidation in rat liver exposed to celecoxib and lansoprazole under epinephrine-induced stress, J. Appl. Pharm. Sci. 7 (2017) 94–99.
[42] P. Kakkar, B. Das, P. Viswanathan, A modified spectrophotometric assay of superoxide dismutase, 1984.
[43] A. Eidi, P. Mortazavi, M. Bazargan, J. Zaringhalam, Hepatoprotective activity of cinnamon ethanolic extract against CCI4-induced liver injury in rats, EXCLI J. 11 (2012) 495–507.
[44] H.S. Parmar, P. Jain, D.S. Chauhan, M.K. Bhinchar, V. Munjal, M. Yusuf, K. Choube, A. Tawani, V. Tiwari, E. Manivannan, DPP-IV inhibitory potential of naringin: an in silico, in vitro and in vivo study, Diabetes Res. Clin. Pract. 97 (1) (2012) 105–111.
[45] M. Ota, P.J. Houghton, Boswellic acids with acetylcholinesterase inhibitory properties from frankincense, Nat. Prod. Commun. 3 (1) (2008), 1934578X0800300105.
[46] N.C. Chaulya, P.K. Haldar, A. Mukherjee, Antidiabetic activity of methanol extract of rhizomes of Cyperus tegetum Roxb.(Cyperaceae), Acta Pol. Pharm. 68 (6) (2011) 989–992.
[47] P. Daisy, J. Eliza, S. Ignacimuthu, Influence of Costus speciosus (Koen.) Sm. Rhizome extracts on biochemical parameters in streptozotocin induced diabetic rats, J. Health Sci. 54 (6) (2008) 675–681.
[48] M. Fowler, Microvascular and macrovascular complications of diabetes, Clin. Diabetes 26 (2) (2008) 77–82.
[49] J.L. Rains, S.K. Jain, Oxidative stress, insulin signaling, and diabetes, Free Radic. Biol. Med. 50 (5) (2011) 567–575.
[50] L.-Y. Li, L.-Q. Li, C.-H. Guo, Evaluation of in vitro antioxidant and antibacterial activities of Laminaria japonica polysaccharides, J. Med. Plants Res. 4 (21) (2010) 2194–2198.
[51] M.S. Balasubashini, R. Rukkumani, P. Viswanathan, V.P. Menon, Ferulic acid alleviates lipid peroxidation in diabetic rats, Phytother. Res. Int. J. Devoted Pharmacol. Toxicol. Eval. Nat. Prod. Deriv. 18 (4) (2004) 310–314.
[52] N. Vardi, H. Parlakpinar, F. Ozturk, B. Ates, M. Gul, A. Cetin, A. Erdogan, A. Otlu, Potent protective effect of apricot and β-carotene on methotrexate-induced intestinal oxidative damage in rats, Food Chem. Toxicol. 46 (9) (2008) 3015–3022.
[53] J. Kasznicki, M. Kosmalski, A. Sliwinska, M. Mrowicka, M. Stanczyk, I. Majsterek, J. Drzewoski, Evaluation of oxidative stress markers in pathogenesis of diabetic neuropathy, Mol. Biol. Rep. 39 (9) (2012) 8669–8678.
[54] M. Kanehisa, Post-genome informatics, OUP Oxford 2000.
[55] A. Daina, O. Michielin, V. Zoete, SwissTargetPrediction: updated data and new features for efficient prediction of protein targets of small molecules, Nucleic Acids Res. 47 (W1) (2019) W357–W364.
[56] A. Gaulton, A. Hersey, M. Nowotka, A.P. Bento, J. Chambers, D. Mendez, P. Mutowo, F. Atkinson, L.J. Bellis, E. Cibrián-Uhalte, The ChEMBL database in 2017, Nucleic Acids Res. 45 (D1) (2017) D945–D954.